JOURNAL GEOLOGICAL SOCIETY OF INDIA
Vol.91, February 2018, pp.135-146

Density, Viscosity and Velocity (Ascent Rate) of Alkaline Magmas

Gaurav J. Kokandakar, Sachin S. Ghodke, K. Rathna, Laxman B. More, B. Nagaraju, Munjaji V. Bhosle and K. Vijaya Kumar*

School of Earth Sciences, SRTM University, Nanded – 431 606, India
***E-mail:** vijay_kumar92@hotmail.com*

ABSTRACT

Three distinct alkaline magmas, represented by shonkinite, lamprophyre and alkali basalt dykes, characterize a significant magmatic expression of rift-related mantle-derived igneous activity in the Mesoproterozoic Prakasam Alkaline Province, SE India. In the present study we have estimated emplacement *velocities (ascent rates)* for these three varied alkaline magmas and compared with other silicate magmas to explore composition control on the ascent rates. The alkaline dykes have variable widths and lengths with none of the dykes wider than 1 m. The shonkinites are fine- to medium-grained rocks with clinopyroxene, phologopite, amphibole, K-feldspar perthite and nepheline as essential minerals. They exhibit equigranular hypidiomorphic to foliated textures. Lamprophyres and alkali basalts characteristically show porphyritic textures. Olivine, clinopyroxene, amphibole and biotite are distinct phenocrysts in lamprophyres whereas olivine, clinopyroxene and plagioclase form the phenocrystic mineralogy in the alkali basalts. The calculated densities [2.54-2.71 g/cc for shonkinite; 2.61-2.78 g/cc for lamprophyre; 2.66-2.74 g/cc for alkali basalt] and viscosities [3.11-3.39 Pa s for shonkinite; 3.01-3.28 Pa s for lamprophyre; 2.72-3.09 Pa s for alkali basalt] are utilized to compute velocities (ascent rates) of the three alkaline magmas. Since the lamprophyres and alkali basalts are crystal-laden, we have also calculated effective viscosities to infer crystal control on the velocities. Twenty percent of crystals in the magma increase the viscosity by 2.7 times consequently decrease ascent rate by 2.7 times compared to the crystal-free magmas. The computed *ascent rates* range from 0.11-2.13 m/sec, 0.23-2.77 m/sec and 1.16-2.89 m/sec for shonkinite, lamprophyre and alkali basalt magmas respectively. Ascent rates increase with the width of the dykes and density difference, and decrease with magma viscosity and proportion of crystals. If a constant width of 1 m is assumed in the magma-filled dyke propagation model, then the sequence of emplacement velocities in the decreasing order is alkaline magmas (4.68-15.31 m/sec) > ultramafic-mafic magmas (3.81-4.30 m/sec) > intermediate-felsic magmas (1.76-2.56 m/sec). We propose that SiO_2 content in the terrestrial magmas can be modeled as a semi-quantitative "geospeedometer" of the magma ascent rates.

INTRODUCTION

The main mechanism of migration of magmas through lithospheric mantle and crust is by propagation of magma-filled cracks i.e. dykes (Shaw, 1980; Spera, 1984; Russell et al., 2012). Dykes allow rapid transport of magma without large scale crystallization *en route*; as a result they represent connecters between regions of melt production and regions of magma accumulation/eruptions. The dykes inject either through pre-existing fractures or create their own pathways by hydraulic fracturing involving dilation of the country rocks. In the field, it is generally observed that fractures do not continue beyond the terminus of the dyke suggesting that magma itself opens fractures to form dykes (see Wada, 1994).

Magma pressure and regional stress field in addition to the host-rock characteristics are the dominant factors that control the length/width ratios, change in orientation, and growth of dykes (Pollard and Muller, 1976). With increasing depth the attitude of the dykes become relatively uniform, but at shallow levels their orientations are controlled by local planes of weakness consequently more irregular dyke patterns are produced. However, different magmas with constant magma pressure emplacing into the same host rocks under similar regional stress conditions show differences in the length/width ratios and thicknesses, suggesting that magma composition also plays a role in the dyke emplacement and growth patterns (Halls and Fahrig, 1987; Ernst et al., 1995). Since viscosity and density of the magmas are controlled by volatiles in addition to the major element chemistry, the emplacement styles of dry and wet magmas with the same bulk-rock compositions are also expected to be different as established by field observation, experiment and theoretical modeling (Pollard et al., 1982; Rogers and Bird, 1987; Olson and Pollard, 1989; Thomas and Pollard, 1993).

Dyke width (a simple measurable quantity in the field) is a significant parameter in understanding and evaluating magma emplacement mechanisms. Magmatic pressure, viscosity, compressive stress acting on dyke plane and elasticity of the host-rock control the width of the dykes and ascent rate of magmas (Pollard, 1987). Dyke width is positively correlated with SiO_2 content and K_2O/MgO ratios (Ui et al., 1984; Wada, 1994). A positive correlation between dyke width and viscosity is also suggested by Wada (1994) thereby implying that felsic dykes would be broader than mafic dykes. However, large mafic dykes (widths >100 m) observed in the Archaean/Proterozoic terrains and Phanerozoic flood basaltic provinces could be due to anomalously high magmatic temperatures related to hotspot activities or any local anomalous thermal conditions (Wada, 1994).

Magma migration in the mantle and crust is essentially buoyancy-driven (Lister and Kerr, 1991). The magma ascent rate is controlled by density difference between magma and ambient crust, speed of crack propagation, and viscosity of the magma (Dingwell and Webb, 1990; Melnik and Sparks, 2005; Whittington et al., 2009). While density difference reflects the scale of buoyancy, volatiles have direct bearing on the crack propagation speed and viscosity of the magma. Magma ascent rates for silicate magmas, which are in the order of < mm/sec to > m/sec, are estimated by using a variety of methods including fluid-filled propagation model, element diffusion profiles in minerals, thickness of mineral growth rims, xenolith settling velocity, dP/dT and dT/dt variation, high-PT experiments and numerical modeling (Spera, 1984; Klügel et al., 1997, Nicholis and Rutherford, 2004; Demouchy et al., 2006; Peslier and Luhr, 2006; Sparks et al., 2006; Mattsson, 2012; Yamato et al., 2012; Armienti et al., 2013; Baruah et al., 2013; Jankovics et al., 2015; Ray et al., 2016). Among the different methods used for calculating magma propagation velocities, it is found that fluid-filled crack propagation model seems to estimate higher ascent rates (Jankovics et al., 2015; Ray et al., 2016).

In the present study an attempt has been made to quantify the

0016-7622/2018-91-2-135/$ 1.00 © GEOL. SOC. INDIA | DOI: 10.1007/s12594-018-0827-8

flow velocities of mafic alkaline magmas on the basis of viscosity, density and width of the dykes using fluid-filled crack propagation model (Spera, 1984; Sparks et al., 2006). The three alkaline mafic magmas considered in this study correspond to the shonkinitic, lamprophyric and alkali basaltic dykes. This dyke activity belongs to the Mesoproterozoic continental rift-related magmatism within the Prakasam Alkaline Province along the SE margin of India. The main objective of the present work is to explain the relationship between dyke morphology, chemistry and velocity (ascent rate) considering alkaline magmas in particular and silicate magmas in general. For this purpose we have (1) measured the widths of shonkinite, lamprophyre and alkali basaltic dykes in the field, (2) measured densities for alkali basaltic dykes, (3) analyzed the dykes for major elements, (4) calculated densities and viscosities based on empirical relationships, (5) estimated the ascent rates for the three types of the alkaline dykes under laminar and turbulent flow conditions, and (6) computed velocities for different silicate magmas to infer composition control on magma ascent rates.

THREE TYPES OF ALKALINE MAGMAS

Alkaline magmas representing small melt fractions are important components of the intraplate mantle-derived magmatic spectrum. In the Prakasam Alkaline Province (PAP), Eastern Ghats belt, SE India (Fig. 1A), a major Mesoproterozoic continental rift-related tholeiitic and alkaline magmatism occurred between 1.35 and 1.2 Ga (Sarkar and Paul, 1998; Upadhyay et al., 2006; Vijaya Kumar et al., 2007; Vijaya Kumar and Leelanandam, 2008; Vijaya Kumar et al., 2011). The PAP represents a rift-zone within thickened continental crust (Ratnakar and Leelanandam, 1989; Vijaya Kumar and Ratnakar, 2001), and follows the broad structural trend of the craton-mobile belt contact (Fig. 1B). At the present level of exposure, the PAP exposes a spectrum of plutonic complexes formed at mid-crustal level (800 to >1000 ºC and ~ 7 kbar; Vijaya Kumar et al., 2007). The province consists of ultramafic-mafic-anorthosite plutons and alkaline intrusives with nepheline syenite as the dominant member (Fig. 1C). The latest igneous episode of Mesoproterozoic magmatism in the PAP is marked by the emplacement of dykes of diverse compositions. Shonkinite, lamprophyre and alkali basalt of alkaline affinity and gabbro of tholeiitic affinity are the four major dyke varieties in the province. Most of the alkali basalt and gabbroic dykes are restricted to the mafic-ultramafic plutons, whereas the shonkinite and lamprophyre dykes are mostly confined to the alkaline complexes. In addition to the four principal types of mafic dykes many unusual dykes including

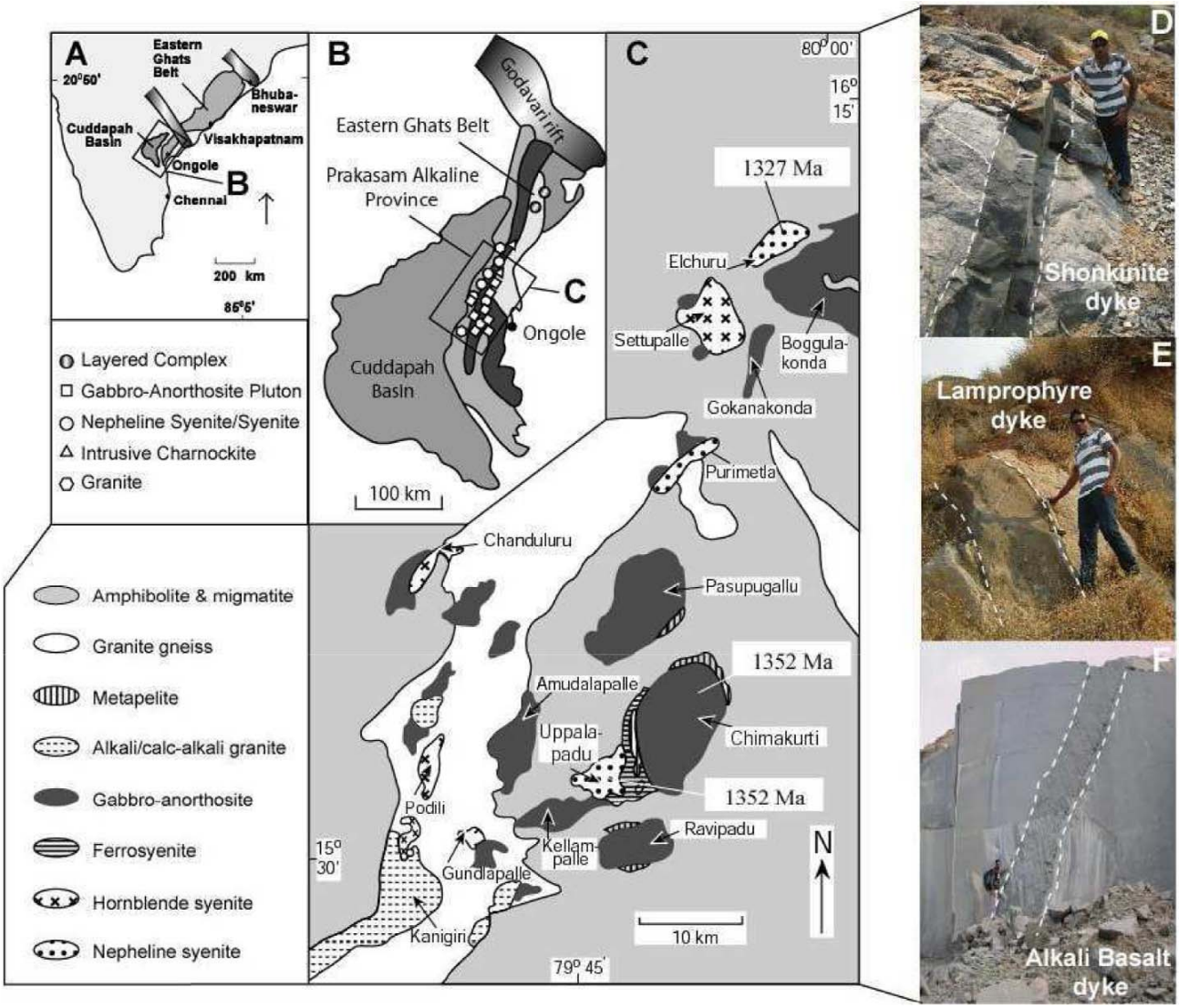

Fig.1. Simplified geological map of the Prakasam Alkaline Province (PAP), Eastern Ghats Belt, SE India (**C**; after Rao et al., 1987; Leelanandam, 1989) showing the distribution of mafic–ultramafic, nepheline syenite and granitoid intrusives. Location of intrusives with respect to the Cuddapah Basin (**B**) and the setting of the Cuddapah Basin and the Eastern Ghats Belt within Peninsular India (**A**) are also shown. Age data are from Upadhyay et al. (2006) and Vijaya Kumar et al. (2007, 2011). Representative shonkinite and lamprophyre dykes from Elchuru alkaline complex (**D** and **E**) and alkali basalt dyke from Chimakurti mafic-ultramafic complex (**F**) are shown.

anorthosite, plagioclase-peridotite and hercynitite among others are reported from the PAP (Babu et al., 1997; Rathna et al., 2000 and references cited therein). Although the dykes are not dated, petrological and geochemical similarities with the host plutons and field features such as sinuosity and off-setting of the dykes suggest that the dyke activity was simultaneous with the host plutons, i.e. belongs to the 1.35-1.2 Ga period rift-related igneous activity (Subba Rao et al., 1989; Rathna et al., 2000; Upadhyay et al., 2006; Vijaya Kumar et al., 2007). Further, these dykes are compositionally similar to melts parental to the plutons they intrude (Vijaya Kumar et al., 2007).

The three alkaline magmas focused in the present study, represented by shonkinite, lamprophyre and alkali basalt dykes, are selected from the Elchuru alkaline complex and Chimakurti mafic-ultramafic complex (Fig. 1D, E and F). The magmas are designated as 'alkaline' based on their mineralogy (modal or normative nepheline) and alkali/silica ratio which is much higher than calc-alkaline and tholeiitic magmas. In the TAS diagram (Le Bas et al., 1986), the analyzed alkaline basalts fall within the field of basalt whereas shonkinite and lamprophyre fall in the fields of tephrite, phonotephrite and tephriphonolite.

The shonkinite dykes are mineralogically and geochemically similar to the host coarse-grained shonkinite of the Elchuru pluton but are fine- to medium-grained; consequently in the literature the shonkinite dykes are designated as "microshonkinites" (Madhavan et al., 1989 and 1992). However, it is prefered to describe the dykes as shonkinites as the focus of the study is on the magma-type but not on grain-size based distinctions. The shonkinite dykes are massive, and trend dominantly in NW-SE with steep to vertical dips. The broken surface of shonkinite dyke imparts shiny appearance due to abundant mica. They show sharp, straight as well as curvilinear contacts with the host nepheline syenites. Length of the dykes varies from 10 to 100 m and width ranges between 10 and 100 cm. The shonkinite dykes exhibit equigranular hypidiomorphic to foliated textures with clinopyroxene, phlogopite, amphibole, K-feldspar perthite and nepheline as the chief minerals (Fig. 2A).

The lamprophyre dykes strike mostly in NE-SW and NW-SE directions and show steep dips. Length of the lamprophyre dykes varies from 10 to 50 m and width is less than a meter. Being characteristically porphyritic, the lamprophyre dykes frequently show pitted appearance due to removal of phenocrystic minerals. The lamprophyres are marked by a variety of phenocrystic mafic minerals set in a groundmass of second generation mafic minerals and feldspar and/or feldspathoid (Fig. 2B). Euhedral phenocrysts of olivine, clinopyroxene, biotite and amphibole define porphyritic and panidiomorphic textures, though all of them may not present in a single dyke. Zoning in clinopyroxene is prominent in the lamprophyres (Fig. 2B).

The alkali basaltic dykes are melanocratic, massive and are fine-grained in nature. The alkali basaltic dykes are marked by characteristic field features such as sinuosity and off-setting patterns. The dykes trend in N-S, E-W and NE-SW with steep dips around 72° to 85°. The alkali basalt dykes have lengths from 5 to >100 m and widths from 20 to 150 cm. Alkali basaltic dykes exhibit porphyritic and glomeroporphyritic textures with phenocrystic assemblages of olivine-clinopyroxene (± plagioclase) and olivine-plagioclase set in a groundmass of plagioclase-clinopyroxene-olivine-biotite-magnetite (Fig. 2C); locally nepheline is present in the groundmass (Madhavan and Mallikharjuna Rao, 1990; Rathna et al., 2000).

Range and average major element composition of the shonkinite, lamprophyre and alkali basalt dykes and the measured width (cm), and calculated density (g/cc), viscosity (Pa s) and velocity (m/sec) are given in Table 1. Most of the shonkinite and lamprophyre dykes are sinuous with variable widths. The dyke width presented in the Table 1 and used in the calculations is the maximum measured width of an exposed dyke. Range and average widths are given only for chemically analyzed dykes (Table 1) but not all the dykes observed in the field. All the dykes considered in the present study have widths less than 1 m. The measured widths are 15.24-68.73 cm, 21.34-77 cm and 45.35-76.34 cm for shonkinite, lamprophyre and alkali basalt dykes respectively (Table 1). Based on the varied length/width ratios, the three types of dykes are classified into 'mini dykes' (width is less than

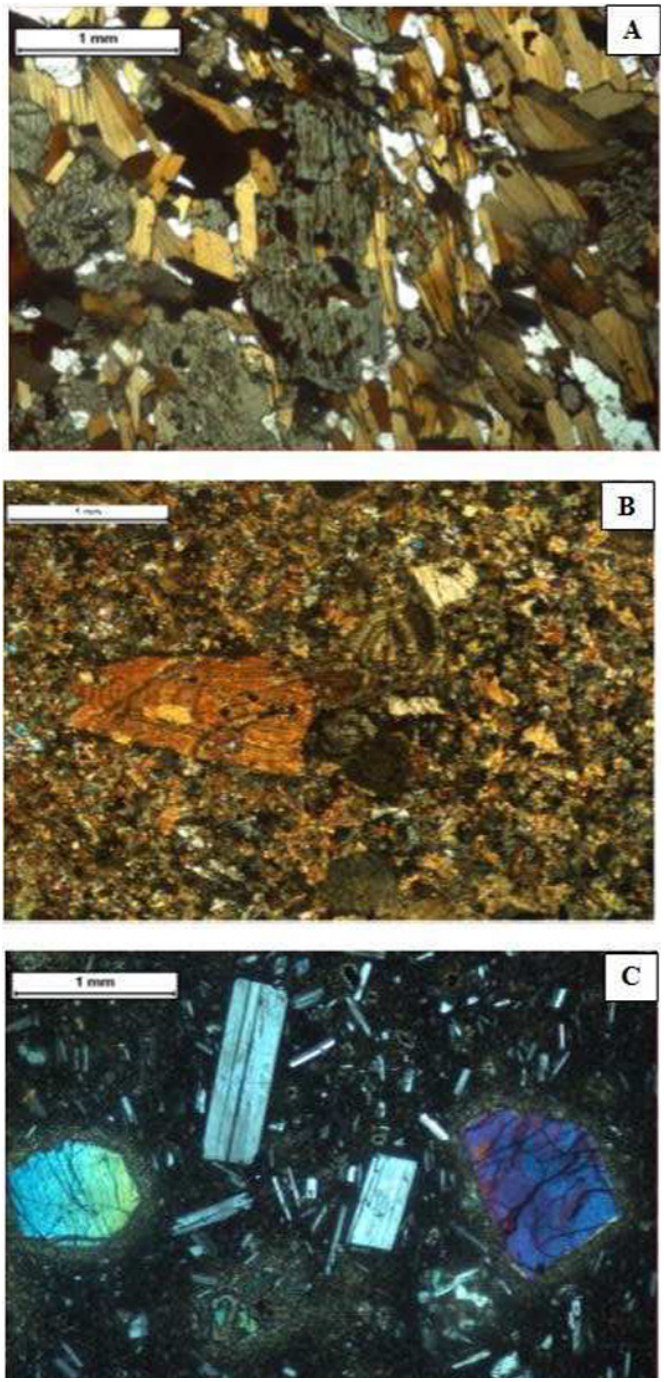

Fig.2. Photomicrographs of shonkinitic (**A**), lamprophyric (**B**) and alkali basaltic (**C**) dykes from the Prakasam Alkaline Province. (**A**) The shonkinite dyke is equigranular hypidiomorphic to foliated with clinopyroxene, biotite, amphibole, K-feldspar perthite and nepheline as the chief minerals; (**B**) the lamprophyre dyke with euhedral to subhedral olivine and clinopyroxene phenocrysts set in a groundmass of K-feldspar-biotite-magnetite. Note concentric zoning in clinopyroxene; (**C**) the alkali basalt dyke with phenocrysts of euhedral olivine and plagioclase set in a groundmass composed of plagioclase-clinopyroxene-olivine-biotite-magnetite. Length of the bar is 1 mm in all the photomicrographs.

Table 1. Range and average major element composition (wt.%), width, density, viscosity and velocity data for the alkaline dykes from the Prakasam Alkaline Province, Eastern Ghats Belt, SE India

	Shonkinite dykes *[N = 28]*			Lamprophyre dykes *[N = 17]*			Alkali basalt dykes *[N = 21]*		
	Range			Range			Range		
	Min.	Max.	Avg.	Min	Max	Avg.	Min	Max	Avg.
SiO_2	44.28	53.86	47.68	43.38	50.68	45.69	43.98	50.23	45.93
TiO_2	0.83	4.38	2.78	1.39	2.89	2.20	1.14	3.25	1.83
Al_2O_3	10.14	16.58	12.56	9.41	17.52	14.07	10.05	16.66	14.62
FeO^t	7.55	12.24	10.57	6.50	16.44	9.74	7.21	13.32	11.01
MnO	0.13	0.21	0.17	0.04	1.07	0.28	0.12	0.21	0.17
MgO	5.08	10.46	8.00	5.01	19.93	8.62	5.71	14.13	9.22
CaO	3.15	8.91	6.66	5.55	10.05	8.42	7.20	12.25	11.03
Na_2O	1.42	5.16	2.92	1.80	5.84	3.86	1.36	4.45	2.68
K_2O	1.77	6.33	5.27	1.45	6.91	4.46	0.38	2.07	1.28
P_2O_5	0.37	1.68	1.06	0.36	0.96	0.60	0.01	0.90	0.13
Width (cm)	15.24	68.73	41.98	21.34	77.00	49.17	45.35	76.34	60.84
Density (g/cc)	2.54	2.71	2.63	2.61	2.78	2.68	2.66	2.74	2.71
Viscosty (Pa s) @ 1000 ^oC	3.11	3.39	3.27	3.01	3.28	3.12	2.72	3.09	2.83
Velocity (m/sec) @ $\Delta\rho$ = 100 kg/m^3	0.11	2.13	0.83	0.23	2.77	1.19	1.16	2.89	2.00
Velocity (m/sec) @ $\Delta\rho$ = 200 kg/m^3	0.23	4.27	1.65	0.46	5.54	2.37	2.32	5.78	4.01
Velocity (m/sec) @ $\Delta\rho$ = 300 kg/m^3	0.34	6.40	2.48	0.70	8.30	3.56	3.47	8.66	6.01

Deatails of density, viscosity and velocity calculations are given in the text.

10 cm) and 'macro dykes' (width between 10 and 100 cm) (Bird et al., 1985). Average density of alkali basalt (2.70 g/cc) is slightly greater than that of lamprophyre (2.68 g/cc) and shonkinite (2.63 g/cc). The average viscosity (at 1000 ^oC) of alkali basalt (2.83 Pa s) is lower than that of lamprophyre (3.12 Pa s) and shonkinite (3.27 Pa s) (Table 1). The ranges of computed velocities (ascent rates) are 0.11-2.13 m/sec, 0.23-2.77 m/sec and 1.16-2.89 m/sec for shonkinite, lamprophyre and alkali basalt magmas respectively. The measured widths of the three types of dykes is used in the calculation of ascent rates. The average velocity of alkali basalt (2 m/sec) is higher than that of lamprophyre (1.19 m/sec) and shonkinite (0.83 m/sec) at $\Delta\rho$ = 100 kg/m^3 (see Table 1).

DENSITY

Density determines the melt buoyancy with respect to ambient pressure gradients. The density contrast between silicate melts and surrounding crust determines the velocity and duration of melt transport. Density increases in melts with depth due to increasing compressibility. There are instances of melt migrating downwards, especially at crust-mantle boundaries, due to negative (ρ_r-ρ_m) density contrast (Arndt, 2013). Water has significant affect on the melt densities. H_2O decreases the density of silicate liquids due to its lower molecular mass but presence of water increases the compressibility thereby off-setting the former effect. However, at crustal depths density does decrease due to presence of H_2O (Jing and Karato, 2012).

The bulk densities (ρ; in g/cc) of the three alkaline magmas are calculated using Bottinga and Weill (1970) method based on partial molar volumes of the major oxides.

$$\rho_m(P,T,X) = \sum_{i=1}^{n} X_i * MW_i / V_i(P,T)$$

Where ρ_m = Density of melt in g/cc; X_i = Mole fraction; MW_i = Molecular weight in g/mol; V = Molar volume in cm^3.

An Excel program (www.whitman.edu/geology/winter/.../CIPW%20Norm%20Hollacher.xls) is used for calculating melt densities. The calculated densities are 2.54-2.71 g/cc, 2.61-2.78 g/cc and 2.66-2.74 g/cc for shonkinite, lamprophyre and alkali basalt dykes respectively (Table 1). These calculated densities are used in estimating the 'ascent rates'. The densities of the alkali basaltic dykes are also measured in order to test the validity of the calculated values. The density measurements are made using 1 inch cores of the fresh alkali basalt dykes on Walker's balance. At least three cores per sample are considered while measuring the densities and the values shown in Figure 3 are average of these three measured values. Since the measured densities are for rocks (solids) and calculated densities are for melts (liquids); the rock densities have been converted to melt densities using the relationship $\rho_{melt} = 0.9 \times \rho_{rock}$. The converted densities are plotted in the Fig.3. A good positive correlation (R^2 = 0.84) between measured and calculated densities indicate that the latter can be utilized in velocity estimations.

VISCOSITY

Viscosity is the prime physical parameter influencing the melt-residue separation in the source region, ascent and emplacement at plutonic depths (Michaut, 2011; Taisne et al., 2011; Michaut et al., 2013) or eruption on the surface (Pinkerton and Stevenson, 1992;

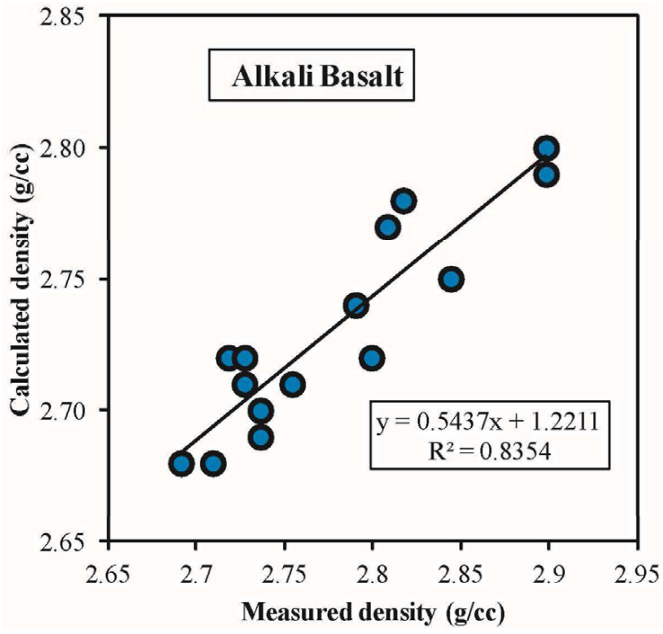

Fig.3. Calculated *versus* measured density (g/cc) in the alkali basalt dykes. See the text for density measurement and calculation procedures.

Dingwell, 1996). The viscosity is a significant factor that controls the magma ascent rates (Sparks, 2003; Dingwell, 2006 and Giordano et al., 2008). A lower viscosity implies faster transport. The viscosity of the silicate magmas vary from 10^{-1} to 10^{14} Pa s (Giordano et al., 2008). Temperature, major element composition, dissolved fluids (especially H_2O and F) and suspended crystals are the main factors that largely modify magma viscosity (up to an order of 10^5; Giordano et al., 2008 and references therein). The viscosity decreases monotonically with increasing temperature. However, the rate of change varies considerably with composition (for example kimberlite *versus* carbonatite; Karki et al., 2013). The decrease is much higher for pure silica melts compared to non-silicate melts. At a temperature of 5000 K viscosities of all the silicate magmas would have similar values. Viscosity-temperature curves are concave-up for all non-Arrhenian silicate melts (Giordano et al., 2008). Hydrous melts tend to be more Arrhenian (linear on η-T graphs) whereas anhydrous melts are more curvilinear on η-T graphs (Giordano et al., 2008). NBO/T (number of non-bridging oxygens per tetrahedral), illustrating the level of polymerization of the melt, is the major compositional control on the viscosity of the silicate magmas. SiO_2, TiO_2, Al_2O_3 and Fe_2O_3 are network formers (Mysen, 1988) and are positively correlated with the viscosities of the magmas. Alkali effect on viscosity is caused by alkali-silica interactions (Fluegel, 2007). Therefore, alkali-rich magmas tend to have higher viscosities then the alkali-poor magmas at comparable SiO_2 contents. However, alkali-rich magmas also contains high H_2O and F contents (positive K-H_2O and K-F relationships; Wada, 1994), therefore the effect of *alkali-silica polymerization* is off-set by hydrous nature of the magma and eventually result in lower viscosities. CO_2, Cl, Br, I and S do not seem to affect the viscosity of silicate magmas (Dingwell and Hess, 1998; Bourgue and Richet, 2001; Zimova and Webb, 2006). Pressure control on the viscosity is complex and depends on the degree of the polymerization of the magma (NBO/T ratio; Bauchy et al., 2013). Viscosity either increases (for melts NBO/T>1) or decreases (for melts NBO/T<1) with increasing pressure (Scarfe et al., 1987). However, pressure control on viscosity seems to be minor compared to temperature and compositional controls at crustal depths (Scarfe et al., 1987; Behrens and Schulze, 2003). Crystallanity or phenocrystic content and lithostatic pressure are other parameters that affect the viscosity of silicate magmas (Bottinga and Weill, 1972; Shaw, 1972; Marsh, 1981; McBirney and Murase, 1984; Dingwell, 1987; Costa, 2005; Giordano et al., 2008; Petford, 2009; Bauchy et al., 2013). Since the alkaline dykes considered in the present study are thin (<1 m), load pressure and time-dependents factor such as ordering polymerization may not be significantly influence the estimated viscosities (Wada, 1994).

Giordano et al. (2008) model has been used to estimate the viscosities for the three alkaline magmas (Table 1; Fig. 4). Giordano et al. (2008) considered composition, temperature and H_2O contents of magma while developing the empirical relationship. The LOI as H_2O has been used in the viscosity calculations. The effective viscosities are also calculated as the lamprophyre and alkali basalt dykes are crystal-laden (porphyritic).

Temperature-dependent viscosity can be modeled by Vogel-Tammann-Fulcher (VTF) equation (Giordano et al., 2008):

$$\text{Log } \eta = A + B/T\,(K) - C$$

Where A is considered as a universal constant for melts of all compositions and B and C are composition dependent parameters (Giordano et al., 2008). An Excel program (http:11www.eos.ubc.Ca/~krussell/VISCOSITY/grdViscosity.html.), where we need to input the whole-rock major element data, is used for the viscosity calculations. Log-viscosity (Pa s) *versus* temperature relationships in the shonkinite, lamprophyre and alkali basalt dykes are shown in Figure 4. Range in the viscosities at liquidus temperatures for shonkinite (~1000 ºC), lamprophyre (~1100 ºC) and alkali basalt (~1200 ºC) are also shown in the Fig.4. Viscosities calculated for all the analyzed dykes at a constant temperature of 1000 ºC are 3.11-3.39 Pa s for shonkinite, 3.01-3.28 Pa s for lamprophyre and 2.72-3.09 Pa s for

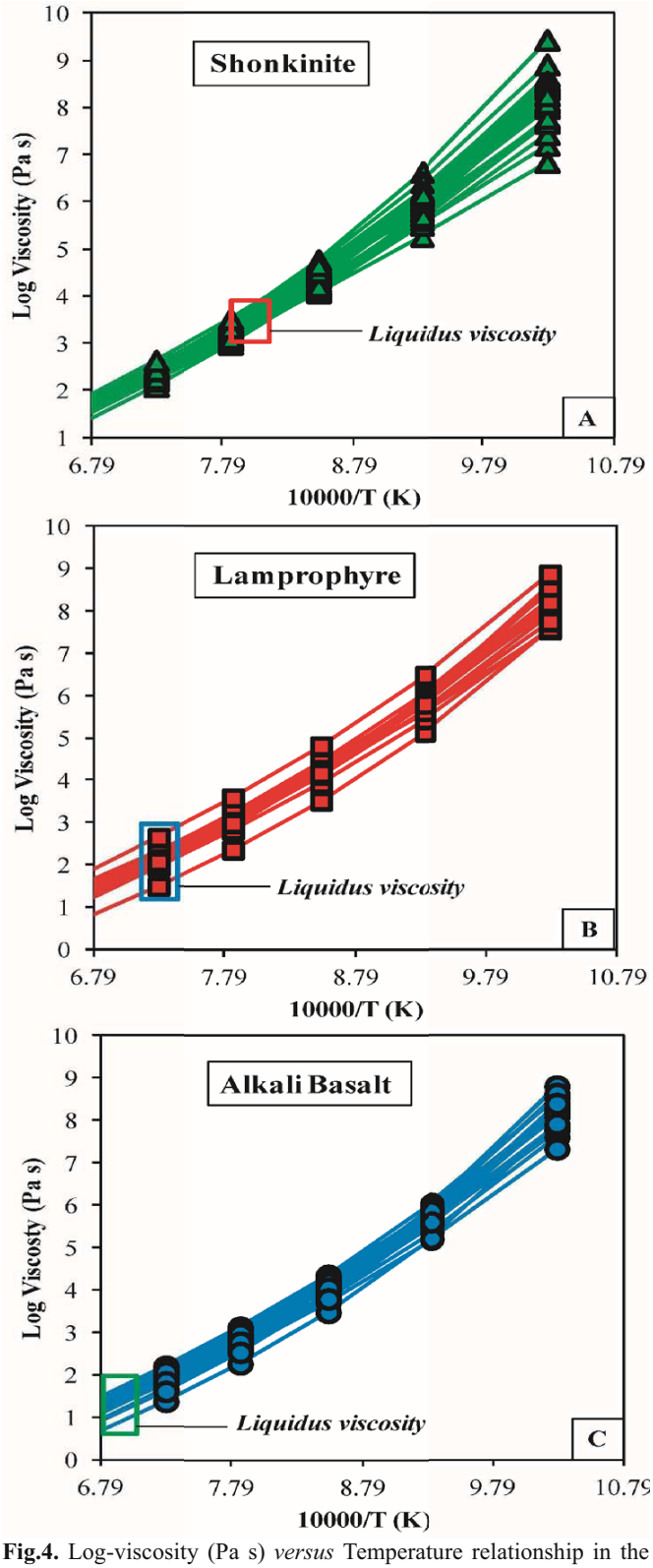

Fig.4. Log-viscosity (Pa s) *versus* Temperature relationship in the shonkinite (**A**), lamprophyre (**B**) and alkali basalt (**C**) dykes. Range in the viscosities at liquidus temperatures (highlighted in boxes) for shonkinite (~1000 ºC), lamprophyre (~1100 ºC) and alkali basalt (~1200 ºC) are shown in the figures. We have used Giordano et al. (2008) method for calculation of viscosities at different temperatures (http//:11www.eos.ubc.Ca/~krussell/VISCOSITY/grdViscosity.html.).

alkali basalt. To detect the effect of water on the melt viscosities, viscosities of shonkinite for anhydrous (H_2O = 0 wt.%) and hydrous (H_2O = 3 wt.%) at constant temperature was calculated . It is found that the viscosities vary by more than a factor of 10 ($10^{3.32}$ Pa s for anhydrous composition and $10^{1.90}$ Pa s with 3.0 wt. % of H_2O). Although the fractures are narrow (less than 1 m), the shonkinite, lamprophyre and alkali basalt magmas could emplace at mid-crustal depths without getting solidified *en route* due to their lower viscosities.

The viscosity of silicate magmas is greatly influenced by the percentage of crystals present in the magmas. The viscosity of the crystal-laden magmas is designated as "effective viscosity" (viscosity of melt + crystal mixture). The lamprophyres and alkali basalts are porphyritic; for this reason, we have also calculated effective viscosities for the lamprophyres and alkali basalts. The presence of crystals essentially increases the viscosities consequently decreases the ascent rates of magmas. Petford (2009) has shown that the percentage of crystals in the magma is the most significant parameter controlling the viscosity of the highly congested (crystal-laden) magmas. Many empirical and theoretical equations are available for calculating effective viscosity (see Table 3 in Petford, 2009). There is little difference in the effective viscosities calculated from different equations (see Table 3 and Fig.7 in Petford, 2009) as long as crystals are < 30%, which is the case for the alkaline magmas of the present study. We have used Einstein-Roscoe (ER) equation as it is commonly used for petrological purposes (see Shaw, 1965; Marsh, 1981). For crystal contents <30% (Shaw, 1965; Arzi, 1978), the main controls on the magmatic viscosity are T, Si and H_2O (Dingwall et al., 1993). Therefore, the effective viscosity calculated using Einstein-Roscoe equation is valid for the alkaline magmas considered here. The effective viscosity of these magmas decreases with increasing temperature but the rate of decrease is less compared to the decrease in the viscosity of pure melt phase. For instance, a 50 °C increase in temperature results in decrease of 0.2 log units in *effective viscosity* but 0.4 log units in the viscosity of pure melt (Caricchi et al., 2007).

$$\eta_E = \eta_o(1-\phi R)^{-2.5} \text{ (Shaw, 1965)}$$

Where η_E = Effective viscosity (Pa s); η_o = Melt viscosity (Pa s); ϕ = Percentage of crystals; R = A constant (1.65; Marsh, 1981)

We have shown the effect of crystals on the viscosity of the lamprophyre and alkali basalt magmas in Fig.5. An exponential increase in viscosity with increasing volume fraction of crystals ($0 < \phi < 0.3$) is evident (Fig. 5). The lamprophyre and alkali basalt dykes contain a maximum of ~20% phenocrysts. A twenty percent of crystals in the lamprophyre and alkali basalt magmas increase the viscosity by 2.7 times compared to the crystal-free magmas (Fig. 5). An abrupt change in slope occurs when $\phi > 0.4$ (Fig. 5). The magmas behave as Newtonian fluids when the percentage of crystals is small, but with increasing proportion of crystals the magmas shift to non-Newtonian behaviour (Kerr and Lister, 1991). The Newtonian to non-Newtonian transition occurs when ϕ = 0.2 to 0.5 (Kerr and Lister, 1991; Petford, 2009) and the system migrates to rigid state when ϕ = 0.6 (Marsh, 1981).

VELOCITY (ASCENT RATE)

The calculation of magma ascent rates made in the present study are based on fluid-filled crack propagation model and assumes that magma ascent in the dykes is mainly buoyancy-driven (Lister and Kerr, 1991). The viscosity calculated at 1000 °C in the mathematical expressions for the estimation of velocities has been used. Such an approach will be expedient in making intra- and inter-dyke comparisons. The calculated velocities are based on simple models which have not considered shear-rate dependence of viscosity, time-dependent effects such as crystal alignment, fractionation and change in melt composition with depth. Similarly, local variations in viscosity due to freezing processes at the walls (Wyllie et al., 1999) and dyke geometry variation in depth (Giberti and Wilson, 1990) are also not considered while calculating the ascent rates.

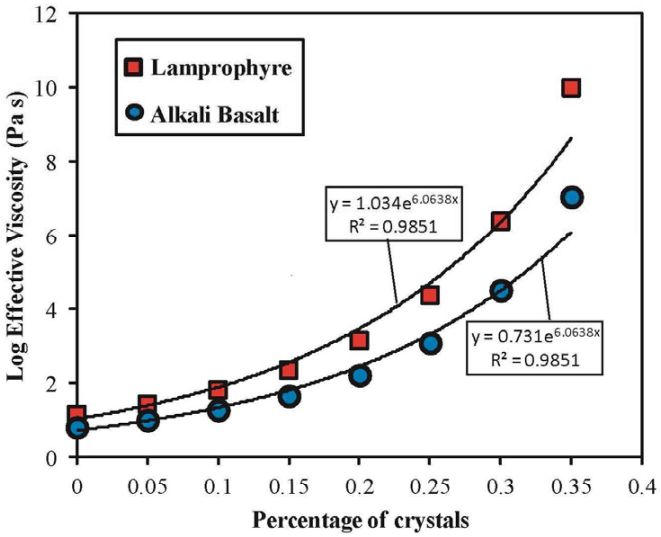

Fig.5. Log effective viscosity (Pa s) *versus* percentage of crystals relationship in the lamprophyre and alkali basalt dykes. We have used average compositions of lamprophyres and alkali basalts in the calculations. Effective viscosity is calculated using the equation $\eta_E = \eta_o(1-\phi R)^{-2.5}$ (Shaw, 1965). Note the exponential relationship between proportion of crystals and effective viscosity.

The calculated the velocities (ascent rates) for the shonkinite, lamprophyre and alkali-basalt alkaline magmas are calculated using three different mathematical equations: equation 1 is used for laminar flow (Sparks, 1993) and equations 2 and 3 for turbulent flow of the magma (Huppert and Sparks, 1985a; Philpotts, 1990; Sparks et al., 2006). The shonkinite, lamprophyre and alkali basalt magmas may have migrated in laminar flow as the width of the dykes is less than 1 meter. For dykes of basaltic composition, the flow tends to be laminar for width up to 8 m (Philpotts, 1990). However, all the three magmas are rich in volatiles consequently have low viscosities suggesting that the magmas might have experienced turbulent flow at least locally. Therefore, the velocities calculated using laminar and turbulent flow equations encompass the possible range of ascent rates for the three alkaline magmas (Table 2).

$$V_E = \Delta\rho g(2W)^2/64\eta \text{ ..... Eq.1 (Sparks, 1993)}$$

Where V_E = Velocity of emplacement (ascent rate) in cm/sec; W = Half-width of the dyke (cm); η = Viscosity of the magma (10 x Pa s) $\Delta\rho$ = Density difference between host rock and magma (ρ_r-ρ_m) (g/cc); g = Acceleration due to gravity (980 cm/sec^2).

$$V_E = 7.7\,[W^5/\{\eta(\rho_m g\Delta\rho)^3\}]^{1/7} g\Delta\rho \text{ .....Eq.2 (Sparks et al., 2006)}$$

Where V_E = Velocity of emplacement (ascent rate) in m/sec; W = Half-width of the dyke (m); η = Magma viscosity (Pa s); ρ_m = Magma density (kg/m^3); $\Delta\rho$ = Density difference between magma and surrounding rocks (ρ_r-ρ_m) (kg/m^3); g = Acceleration due to gravity (9.8 m/sec^2). The factor 7.7 is experimentally determined (Lister and Kerr, 1991).

$$V_E = (\Delta\rho g 2W/k\rho_m)^{1/2} \text{ ..... Eq.3 (Huppert and Sparks, 1985a; Philpotts, 1990)}$$

Where V_E = Velocity of emplacement (ascent rate) in m/sec; W = Half-width of the dyke (m); $\Delta\rho$ = Density difference between magma and surrounding rocks (ρ_r-ρ_m) (kg/m^3); g = Acceleration due to gravity

Table 2. Average velocities (ascent rates) for shonkinite, lamprophyre and alkali basalt dykes based on different equations, widths and density differences

	Width (m)	Shonkinite			Lamprophyre			Alkali Basalt		
		($\Delta\rho$ = 100 kg/m^3)	($\Delta\rho$ = 200 kg/m^3)	($\Delta\rho$ = 300 kg/m^3)	($\Delta\rho$ = 100 kg/m^3)	($\Delta\rho$ = 200 kg/m^3)	($\Delta\rho$ = 300 kg/m^3)	($\Delta\rho$ = 100 kg/m^3)	($\Delta\rho$ = 200 kg/m^3)	($\Delta\rho$ = 300 kg/m^3)
Eq. 1	2w = 1 m	4.68	9.37	14.05	4.91	9.82	14.72	5.41	10.82	16.23
	2w = 0.5 m	1.17	2.34	3.51	1.23	2.45	3.68	1.35	2.71	4.06
	2w = 0.25 m	0.29	0.59	0.88	0.31	0.61	0.92	0.34	0.68	1.01
Eq. 2	2w = 1 m	6.94	10.32	13.01	6.93	10.3	12.99	7.00	10.40	13.11
	2w = 0.5 m	4.23	6.29	7.93	4.22	6.28	7.92	4.26	6.34	7.99
	2w = 0.25 m	2.58	3.83	4.83	2.58	3.83	4.82	2.60	3.86	4.87
Eq. 3	2w = 1 m	6.10	8.63	10.47	6.05	8.55	10.47	6.01	8.50	10.42
	2w = 0.5 m	4.32	6.10	7.48	4.28	6.05	7.41	4.25	6.01	7.37
	2w = 0.25 m	3.05	4.32	5.29	3.02	4.28	5.24	3.01	4.25	5.21

Equation 1: $V_E = \Delta\rho g(2W)^2/64\eta$ (Sparks, 1993)**; Equation 2:** $V_E = 7.7\ [W^5/\{\eta(\rho_m g\Delta\rho)^3\}]^{1/7} g\Delta\rho$ (Sparks et.al, 2006)**; Equation 3:** $V_E = (\Delta\rho g2W/k\rho_m)^{1/2}$ (Huppert and Sparks, 1985a; Philpotts,1990). Parameters in the equations are explained in the text.

(9.8 m/sec^2); *k* = Friction coefficient (varies between 0.01 and 0.06; Huppert and Sparks, 1985a)

During these calculations the following average viscosities: shonkinite = 3.27 Pa s; lamprophyre = 3.12 Pa s; alkali basalt = 2.83 Pa s (Table 1) have been considered. In the equation 3, a friction coefficient of 0.2 has been used as the alkaline magmas tend to have lower friction. Velocities at different dyke widths (2W = 1, 0.5 and 0.25 m) and density differences ($\Delta\rho$ = 100, 200 and 300 kg/m^3) (Table 2) have been calculated. Velocity of the magma is positively correlated with width of dyke, density difference and negatively correlated with viscosity (Table 2). In turbulent flow, the velocity is proportional to square-root of the width, whereas in laminar flow it is proportional to the width squared. The velocities calculated using 3 different equations broadly gave similar results. In the equation 1, the velocities are strongly controlled by widths of the dyke compared to equations 2 and 3 (Table 2). The difference between estimates of velocity by the three equations is not significant when the dyke width is more and $\Delta\rho$ is low but becomes significant when the width is less and $\Delta\rho$ is high. For the given width, the velocities calculated by using equation 1 are > those by equation 2 > those by equation 3 at high $\Delta\rho$ ($\Delta\rho$ = 300 kg/m^3) values. For example, for a 1 m wide alkali basalt dyke with $\Delta\rho$ = 300 kg/m^3, the ascent rates are 16.23 m/sec, 13.11 m/sec and 10.42 m/sec as calculated by equations 1, 2 and 3 respectively (Table 2). However, the velocities almost become equal when width is 1 m and $\Delta\rho$ = 100 kg/m^3 (5 ± 1 m for all the three types of magmas). In the discussions below, the ascent rates calculated based on equation 1 have been used.

Viscosity, crystal content and width control on the velocities of the alkaline magmas are shown in Figs. 6A, 6B and 6C respectively. Exponential decrease in velocity with increasing viscosity is evident (Fig. 6A). We have considered average measured width and average viscosity at given temperature while calculating the velocities. At lower viscosities the dykes with variable widths show large differences in the velocities, but at higher viscosities the differences between the velocities are much smaller (Fig. 6A). Presence of crystals drastically affects the emplacement velocities of the dykes. The velocity of the dykes with variable percentages of crystals (phenocrysts) in the magma have been calculated. A negative exponential relationship is obvious (Fig. 6B). Since the alkali basalts and lamprophyres are phenocryst-laden, their effective viscosities would be higher consequently the ascent rates would be lower (Fig. 6B; Yamato et al., 2012). The final emplacement velocities for the alkali basalt and lamprophyre dykes with 20% crystals may be 2.7 times slower compared to the calculated velocities assuming crystal-free magmas (Fig. 6B). The measured width of the dyke is positively correlated with the estimated velocity in all the three alkaline magmas (Fig. 6C). The computed ascent rates based on measured widths and at $\Delta\rho$ = 100 kg/m^3 (Table 1) range from 0.11 to 2.13 m/sec, 0.23 to 2.77 m/sec and 1.16 to 2.89 m/sec for shonkinite, lamprophyre and alkali basalt magmas respectively (Table 1; Fig. 6C). The ascent rates decrease in the order: alkali basalts (average velocity = 2 m/sec) > lamprophyre (average velocity = 1.19 m/sec) > shonkinite (average velocity = 0.83 m/sec) (Tables 1 and 2; Fig. 6).

ALKALINE MAGMA: A RAPID "MAIL" FROM THE MANTLE

Magma ascent rates for silicate magmas range from 26 km/day for xenoliths-bearing magmas (Blatter et al., 1998) to as low as 10 km/yr for silica-rich magmas (McKenzie, 2000). Carbonatite magmas are possibly the most rapidly ascending terrestrial magmas with ascent rates of 20-60 m/sec (Genge et al., 1995). Kimberlite ascents at a speed >4 to 20 m/sec (Spera, 1984; Sparks et al., 2006) through a 1 m wide conduit especially at dyke stage (Wilson and Head, 2007); thus take ~ 0.23 to 2.32 days to travel ~ 200 km distance and emplace within the shallow continental crust (Wartho and Kelley, 2003; Downes et al., 2006). An ascent rate as high as 40 m/sec (Peslier and Luhr, 2006; Peslier et al., 2008) is also proposed for kimberlitic magmas. Based on kinetics of diamond-graphite transition, settling velocity of diamond phenocrysts in magma, and finite element modeling of dynamics of tensile failure, Barauh et al. (2013) proposed rapid ascent of diamond-bearing kimberlitic magmas. Barauh et al. (2013) suggested that if the kimberlite magmas transport at velocities < 3 m/s then 90% of diamond would be converted to graphite; whereas if the velocities are > 10 m/s then only 10% of diamond would be converted to graphite. It is evident that the speed of ascent controls the retention of diamonds in kimberlites. Ascent rates of olivine mellilite magmas range between 8.5 and 36 m/sec (Mattsson, 2012). Rates of ascent for alkaline magmas range between cm/sec to m/sec depending on the fracture width, fracture resistance, pressure gradient and melt viscosity (Spera, 1984, 1986). Mafic alkaline magma ascent rates are found to be on the order of 0.2 to 8 m/sec based on H diffusion in olivine (Demouchy et al., 2006; Peslier and Luhr, 2006). The xenoliths-bearing Deccan alkali basaltic dykes have ascent velocities of 1.63-8.39 m/sec. Kimberlite ascent rates are faster than alkali basalt, alnoite and lamproite magmas (Kelley and Wartho, 2000; Peslier et al., 2008). Komatiite magma, with low viscosities of 0.1 to 10 Pa s, ascents under turbulent flow conditions at a rate of 1 to 10 m/sec (Huppert and Sparks, 1985b). Basalts have ascent rates of 3 x 10^{-3} to 0.5 m/sec and trachy basalts ascent at 0.3 x 10^{-3} m/sec to 0.42 x 10^{-3} m/sec (Pollard et al., 1983; Armienti et al., 2013; Jankovics et al., 2013). Based on amphibole breakdown, an ascent rate of 4 x 10^{-3} to 18 x 10^{-3} m/sec was estimated for dacite magmas (Rutherford and Hill, 1993). Based on

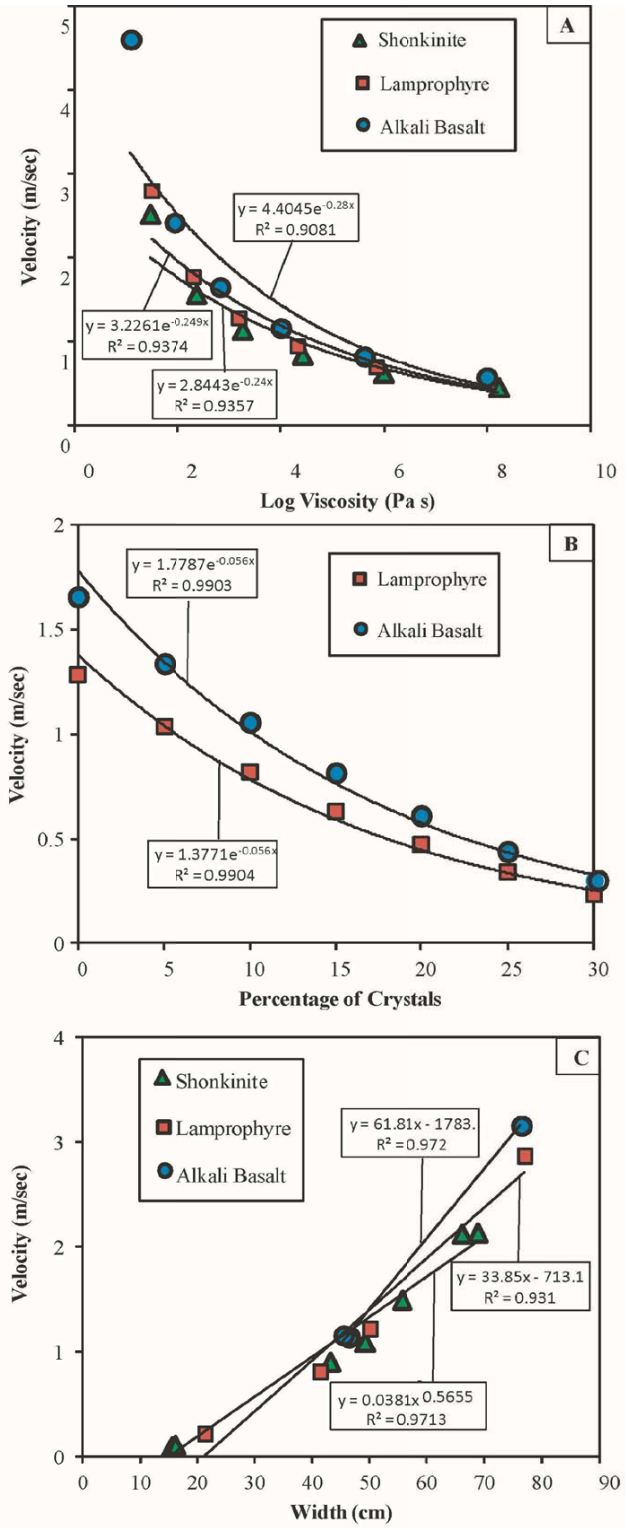

Fig.6. Velocity (cm/sec) *versus* Log viscosity (Pa s) relationship for the shonkinite, lamprophyre and alkali basalt dykes (**A**). We have used the equation $V_E=\Delta\rho g(2W^2)/64\eta$ (Sparks, 1993) and measured widths for the calculation of velocities. $\Delta\rho$ is considered as 100 kg/m^3. For details, see the text. Velocity (m/sec) *versus* percentage of crystals relationship for shonkinite, lamprophyre and alkali basalt dykes (**B**). The shonkinite dykes, which possibly represent pure melt composition (0% crystals), may have ascent rates up to 2.5-3.0 m/sec whereas the lamprophyre and alkali basalt dykes with 10-20% crystals may have velocities of 0.5-0.8 m/sec and 0.6-1.1 m/sec respectively. Velocity (m/sec) *versus* measured width (cm) relationship for the shonkinite, lamprophyre and alkali basalt dykes (**C**). A positive relationship is evident for all the three dykes.

decompression experiments, it is found that hawaiites emplace with a velocity of > 0.04 m/sec (Nicholis and Rutherford, 2004). The dominant control of width on the emplacement velocities of mafic and felsic magmas come from modeling of subduction-zone magmas. It has been shown that the hydrous subduction-related mafic and felsic magmas take ~1 hour (an ascent rate of 27.78 m/sec) and 2 years (an ascent rate of 0.0016 m/sec) respectively to flow a 100 km vertical distance through 1 m wide cracks. If the cracks are 1 mm, then the time intervals would be 130 years (an ascent rate of 25 x 10^{-6} m/sec) and 1.6 Ma (an ascent rate of 10^{-10} m/sec) for mafic and felsic melts respectively (Hack and Thompson, 2011). However, some of the granitic dykes have emplacement velocities as high as 5-6 m/sec (Branigan, 1989).

We have calculated ascent rates of different magmas using fluid-filled fracture propagation model in order to evaluate composition control on emplacement velocities. Major element chemistry and calculated viscosity and velocity data for different magmas are given in Table 3. We have considered a constant dyke width of 1 m, and temperature of 1000 °C for the calculation of viscosities, densities and ascent rates (Table 3). Major element data for the shonkinite, lamprophyre and alkali basalt are from the present study and compositions of all other magmas are compiled from the literature (data sources are given in the foot note to Table 3). The viscosities of carbonatite and kimberlite magmas are assumed to be 1 and 2 Pa s where as viscosities of all the other magmas are calculated using Giordano et al. (2008) empirical relationship (Table 3). It is evident that viscosities of intermediate-felsic magmas are > ultramafic-mafic magmas > alkaline magmas (Table 3). We have assumed that all the magmas to be crystal-free. Emplacement velocities for different magmas are calculated at different $\Delta\rho$ values using equation 1 (laminar flow), as we have assumed 1 m dyke width for all the magmas (Fig. 7). By using the liquidus viscosities, the absolute velocities change but the relative positions of the magmas in Fig. 7 do not change, except picrite and komatiite, whose velocities would be higher than alkali

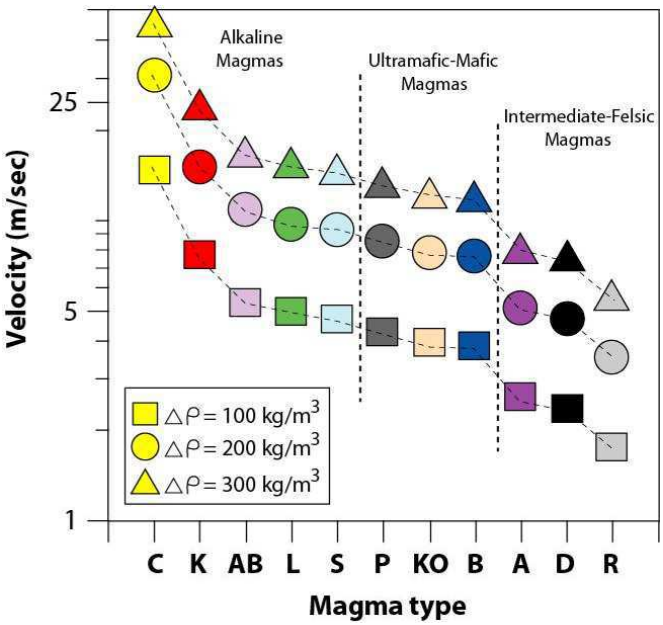

Fig.7. Silicate magma ascent rates (m/sec) estimated at different $\Delta\rho$ values. The parameters considered for calculation of ascent rates are given in Table 3. We have used the equation $V_E=\Delta\rho g(2W^2)/64\eta$ (Sparks, 1993) for calculation of the velocities. Emplacement velocities increase with increasing density difference ($\Delta\rho$). **C** = Carbonatite; **K** = Kimberlite; **AB** = Alkali basalt; **L** = Lamprophyre; **S** = Shonkinite; **P** = Picrite; **KO** = Komatiite; **B** = Basalt; **A** = Andesite; **D** = Dacite; **R** = Rhyolite. See the text for details.

Table 3. Average major element composition (in wt.%), temperature and dyke width data considered for calculating density, viscosity and velocity (ascent rate) for different magmas

	Alkaline magmas					Ultramafic-Mafic magmas			Intermediate-Felsic magmas		
Rock type	Carbonatite	Kimberlite	Alkali Basalt	Lamprophyre	Shonkinite	Picrite	Komatiite	Basalt	Andesite	Dacite	Rhyolite
Data source	1	2	3	4	5	6	7	8	9	10	11
SiO_2	5.53	27.6	45.93	45.69	47.68	43.8	46.75	49.47	59.81	63.4	74.24
TiO_2	0.32	1.6	1.83	2.2	2.78	3.12	0.4	1.08	0.74	0.52	0.31
Al_2O_3	0.49	3.2	14.62	14.07	12.56	12.47	7.31	14.05	17.12	16.6	13.63
FeO[t]	23.92	7.56	11.01	9.74	10.57	12.26	11.18	11.04	6.18	5.78	2.33
MnO	2.61	0.1	0.17	0.28	0.17	0.21	0.18	0.19	0.14	0.15	0.1
MgO	4.05	24.3	9.22	8.62	8	11.09	25.83	7.64	3.13	2.26	0.35
CaO	19.4	14.1	11.03	8.42	6.66	10.67	7.48	12.34	6.8	5.78	1.72
Na_2O	0.13	0.2	2.68	3.86	2.92	3.29	0.54	2.08	3.36	3.41	4.42
K_2O	0.04	0.8	1.28	4.46	5.27	1.43	0.04	0.12	1.5	1.46	2.82
P_2O_5	7.05	0.5	0.13	0.6	1.06	0.73	0.2	0.09	0.17	0.12	0.05
H_2O	0.50	7.9	1.69	1.38	1.8	0.38	0.20	0.34	0.29	0.3	0.29
Temperature (°C)	1000	1000	1000	1000	1000	1000	1000	1000	1000	1000	1000
Width (cm)	100	100	100	100	100	100	100	100	100	100	100
Density (kg/m^3)	2500	3100	2710	2680	2630	2750	2810	2720	2550	2520	2400
Viscosity (Pa s)	1[a]	2[b]	2.83	3.12	3.27	3.56	3.92	4.02	5.97	6.41	8.72
Velocity (Δρ = 100 kg/m^3)	15.31	7.66	5.41	4.91	4.68	4.30	3.91	3.81	2.56	2.39	1.76
Velocity (Δρ = 200 kg/m^3)	30.63	15.31	10.82	9.82	9.37	8.60	7.81	7.62	5.13	4.78	3.51
Velocity (Δρ = 300 kg/m^3)	45.94	22.97	16.23	14.72	14.05	12.90	11.72	11.43	7.69	7.17	5.27

Data souces: **1**: Bühn and Rankin (1999); **2**: Price et al., (2000) and refereces theirin; **3**, **4** and **5**: Present study; **6**: analysis s2-1367 from Fuster et al. (1966); **7**: Nisbet et al. (1993); **8**: Fitton and Godard (2004); **9**: Average of the data from Pearce et al. (1995); Zellmer et al. (2003); Feeley and Davidson (1994); **10**: Lindsay et al. (2005); **11**: Price et al. (2005). a and b: values are assumed.

basalt, lamprophyre and shonkinite magmas.

The calculated velocities at different Δρ values, with respect to magma-type are shown in Fig.7. The velocities of emplacement for all the magmas increase with increasing density difference between the magma and the ambient crust. At a constant dyke width of 1 m carbonatite magmas ascent rapidly (15.3-45.9 m/sec) followed by kimberlite (7.7-23 m/sec), alkali basalt (5.4-16.2 m/sec), lamprophyre (4.9-14.7 m/sec) and shonkinite magmas (4.7-14 m/sec). The three alkaline magmas considered in the present study almost have comparable ascent rates. The ultramafic-mafic magmas have ascent rates (3.8-4.3 m/sec) between alkaline and intermediate-felsic magmas. The intermediate-felsic magmas have the lowest ascent rates (1.8-2.6 m/sec) among the different silicate magmas when the width of the dyke is considered 1 m. However, it is to be noted that felsic magmas require a width of 2-20 m to emplace as dykes without getting solidified en route (Petford et al., 1994). The calculated velocities for the intermediate-felsic magmas are slightly on higher side compared to the ones obtained from amphibole rim growth (Rutherford and Hill, 1993) but are lower than the ones proposed by Branigan (1989; ~5-6 m/sec).

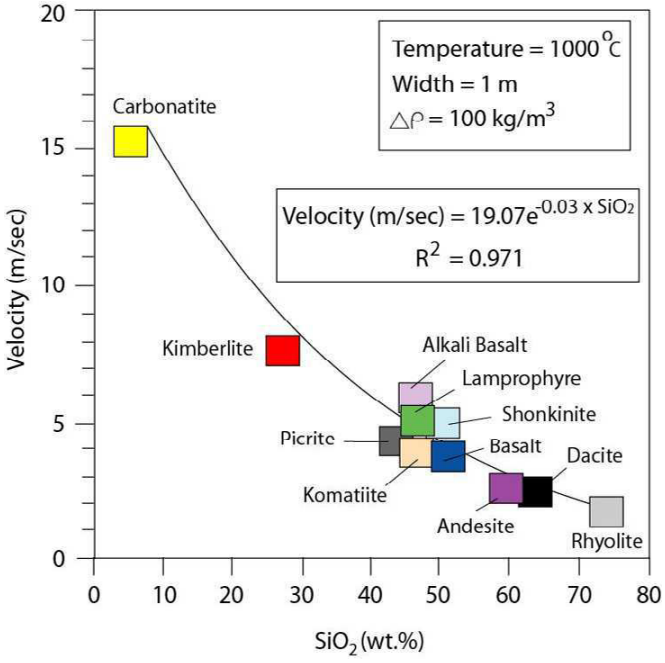

Fig.8. Velocity (m/sec) *versus* SiO_2 (wt.%) relationship in different magmas. Regression equation with correlation coefficient (R^2 value) is shown in the figure. We propose that SiO_2 content in the magma can be used as a semi-quantitative "geospeedometer" of magma ascent rates. Parameters considered in the calculations are given in the Figure and in Table 3.

Time scales of magmatic processes, such as ascent rates, are varied depending on the tool of investigation and its sensitivity (Hawkesworth et al., 2004). Different methods of estimation may yield different ascent rates. For example, estimated ascent rates for xenoliths and xenocryst-bearing alkaline basaltic magmas are in the order of 3.9-15.9 m/s (based on fluid-filled crack propagation models), 0.19 m/sec (based on Ca profiles of olivine xenocrysts), 0.10-0.41 m/sec (based on settling rate of large xenoliths) and 11.9 m/sec (based on dissolution of orthopyroxene xenocrysts) (see Jankovics et al., 2015). Based on the present study we estimate that the time scale for the ascent of alkaline magmas from mantle to crustal depths through fluid-filled crack propagations is in the order of few hours to few days (at a minimum ascent rate of 1 ± 0.5 m/sec to a maximum of 5 ± 1 m/sec).

IS SILICA CONTENT IN THE MAGMAS A "GEOSPEEDOMETER" OF ASCENT RATES?

We have correlated the velocities (calculated at 1 m dyke widths, viscosities at constant temperature of 1000 °C and Δρ values = 100 kg/m^3) with silica contents of the different magmas (Table 3; Fig. 8). A negative exponential relationship between silica and velocity of the magmas [velocity (m/sec) = $19.07e^{-0.03 \times SiO_2 (wt.\%)}$] is evident (Fig. 8).

Increasing the Δρ values results in exactly the same relationship, however, estimates higher ascent rates. Estimation of velocities based on liquidus viscosities also retains the negative exponential relationship between silica and velocity but with a lower correlation coefficient. The silica-velocity graph conspicuously brings out the dominant control of silica on the ascent rates of magmas. The inverse relationship obtained in SiO_2-velocity graph is essentially due to significant control of SiO_2 on the melt viscosities. Higher the silica in the magma higher the viscosity and lower the velocity. The carbonatite with 5.5 wt.% of silica has an emplacement velocity of 15.3 m/sec and kimberlite with 28% silica has an ascent rate of 7.7 m/sec; alkaline and ultramafic-mafic magmas with SiO_2 between 43 and 50 wt.% have velocities of 3.8 to 5.4 m/sec; intermediate magmas (andesite and dacite) with silica contents of 60-63 wt.% ascent to the surface with velocities of ~2.4 ± 1 m/sec; rhyolite (SiO_2 = 74 wt.%) is the "snail" among the silicate magmas (velocity = 1.76 m/sec). It is evident that the SiO_2 content of the magma can be used as semi-quantitative "geospeedometer" of ascent rates. We believe that this provisional correlation established in the present study will form a basis for proposing an empirical mathematic relationship between silica contents and emplacement velocities of the terrestrial magmas.

CONCLUSIONS

1 Three types of alkaline magmas, corresponding to shonkinite, lamprophyre and alkali basalt dykes, from the Mesoproterozoic Prakasam Alkaline Province, SE India, offer clues on the emplacement of silica-poor and volatile-rich magmas.
2 Although the fractures are narrow (less than 1 m), the shonkinite, lamprophyre and alkali basalt magmas could emplace at mid-crustal depths without getting solidified *en route* due to their lower viscosities.
3 The emplacement velocities of the magmas are controlled by width of the fracture, viscosity of the magma, density difference between magma and the ambient crust, and proportion of crystals in the magma.
4 At comparable widths, the alkaline magmas emplace faster than ultramafic-mafic magmas and intermediate-felsic magmas.
5 The SiO_2 content in the terrestrial magmas can be modeled as a semi-quantitative "geospeedometer" of the magma ascent rates.
6 The SiO_2-velocity relationship developed in the present study provide theoretical framework for future studies to understand relationships between dyke morphology, chemistry and the physics of magma emplacement.

Acknowledgements: The DST (Research project to KVK; EMR/2014/000779), UGC (Post Doctoral Fellowship to KR), CSIR (Senior Research Fellowship to SSG) and DST-INSPIRE (Fellowship to GJK, LBM, BN, and MVB) funded this work. The School of Earth Sciences, SRTM University has made available the microscope facility procured under DST-FIST scheme. Dr. Krishna Deshpande measured the densities of alkali basalts. An anonymous journal reviewer offered constructive comments. We gratefully acknowledge the above-mentioned organizations and people for their support.

References

Armienti, P., Perinelli, C. and Putirka, K.D. (2013) A new model to estimate deep-level magma ascent rates, with applications to Mt. Etna (Sicily, Italy). Jour. Petrol., v.54, pp.795-813.

Arndt, N. (2013) The formation massif anorthosite: petrology in reverse. Geosci. Frontiers, v.4, pp.195-198.

Arndt, N.T., Naldrett, A.J. and Pyke, D.R. (1977) Komatiitic and iron-rich tholeiitic lavas of Munro Township, Northeast Ontario. Jour. Petrol., v.18, pp.319-369.

Arzi, A.A. (1978) Critical phenomena in the rheology of partially melted rocks. Tectonophysics, v.44, pp.173-184.

Babu, E.V.S.S.K., Vijaya Kumar, K. and Pyle, D.M. (1997) Spinel (hercynite) adcumulate from the Chimakurti gabbro-anorthosite pluton, Prakasam District, Andhra Pradesh, India: evidence for plagioclase buoyancy and magma mixing. Curr. Sci., v.73, pp.441-444.

Bauchy, M., Guillot, B., Micoulaut, M. and Sator, N. (2013) Viscosity and viscosity anomalies of model silicates and magmas: a numerical investigation. Chem. Geol., v.346, pp.47-56.

Barauh, A., Gupta, A.K., Mandal, N. and Singh, R.N. (2013) Rapid ascent conditions of diamond-bearing kimberlitic magmas: findings from high pressure-temperature experiments and finite element modeling. Tectonophysics, v.594, pp.13-26.

Behrens, H. and Schulze, F. (2003) Pressure dependence of melt viscosity in the system $NaAlSi_3O_8$-$CaMgSi_2O_6$. Amer. Mineral., v.88, pp.1351-1363.

Bird, D.K., Rosing, M.T., Manning, C.E. and Rose, M.N. (1985) Geological field studies of the Miki fjord area, East Greenland. Bull. Geol. Soc. Denmark., v.34, pp.219-236.

Blatter, D.L. and Carmichael, I.S.E. (1998) Hornblende peridotite xenoliths from central Mexico reveal the highly oxidized nature of subarc upper mantle. Geology, v.26, pp.1035-1038.

Bottinga, Y. and Weill, D.F. (1970) Densities of liquid silicate systems calculated from partial molar volumes of oxide components. Amer. Jour. Sci., v.269, pp.169-182.

Bottinga, Y. and Weill, D.F. (1972) The viscosity of magmatic silicate liquids: a model for calculation. Amer. Jour. Sci., v.272, pp.438-475.

Bourgue, E. and Richet, P. (2001) The effects of dissolved CO_2 on the density and viscosity of silicate melts: a preliminary study. Earth Planet. Sci. Lett., v.193, pp.57-68.

Branigan, N.P. (1989) Internal deformation, flow profiles and emplacement velocities of granitic dykes, southwestern Finland. Lithos, v.22, pp.199-211.

Bühn, B. and Rankin, A.H. (1999) Composition of natural, volatile-rich Na-Ca-REE-Sr carbonatitic fluids trapped in fluid inclusions. Geochim. Cosmochim. Acta, v.63, pp.3781- 3797.

Caricchi, L., Burlini, L., Ulmer, P., Gerya, T., Vassalli, M. and Papale, P. (2007) Non-Newtonian rheology of crystal-bearing magmas and implications for magma ascent dynamics. Earth Planet. Sci. Lett. v.264, pp.402-419.

Costa, A. (2005) Viscosity of high crystal content melts: dependence on solid reaction. Geophys. Res. Lett., v.32, doi**:** 10.1029/2005GL024303

Demouchy, S., Jacobsen, S.D., Gaillard, F. and Stern, C.R. (2006) Rapid magma ascent recorded by water diffusion profiles in olivine from Earth's mantle. Geology, v.34, pp.429-432.

Dingwall, D.D., Bagdassarov, G.Y., Bussod, G.Y. and Webb, S.L. (1993) Magma rheology. Mineral. Assoc. Canada, Short Course Handbook on Experiments at high pressure and applications to the Earth's mantle, v.21, pp.131-196.

Dingwell, D.B. (1987) Melt viscosities in the system $NaAlSi_3O_8$-H_20-F_20_{-1}. *In:* Mysen, B.O. (Ed.), Magmatic Processes: Physicochemical Principles. Spec. Publ. Geochem. Soc., v.1, pp. 423-431.

Dingwell, D.B. (1996) Volcanic dilemma: flow or blow? Science, v.273, pp.1054-1055.

Dingwell, D.B. (2006) Transport properties of magmas: diffusion and rheology. Elements, v.2, pp.281-286.

Dingwell, D.B. and Hess, K.U. (1998) Melt viscosities in the system Na–Fe–Si–O–F–Cl: contrasting effects of F and Cl in alkaline melts. Amer. Mineral., v.83, pp.1016-1021.

Dingwell, D.B. and Webb, S.L. (1990) Relaxation in silicate melts. Europe. Jour. Mineral., v.2, pp.427-449.

Downes, P.J., Wartho, J.A. and Griffin, B.J. (2006) Magmatic evolution and ascent history of the Aries micaceous kimberlite, Central Kimberley Basin, Western Australia: evidence from zoned phlogopite phenocrysts, and UV laser $^{40}Ar/^{39}Ar$ analysis of phlogopite–biotite. Jour. Petrol., v.47, pp.1751-1783.

Ernst, R.E., Head, J.W., Parfitt, E.A., Grosfils, E. and Wilson, L. (1995) Giant radiating dyke swarms on Earth and Venus. Earth Sci. Rev., v.39, pp.1-58.

Feeley, T.C. and Davidson, J.P. (1994) Petrology of calc-alkaline lavas at Volcan Ollagüe and the origin of compositional diversity at central Andean stratovolcanoes. Jour. Petrol., v.35, pp.1295-1340.

Fitton, J.G. and Godard, M. (2004) Origin and evolution of magmas on the Ontong Java Plateau. *In:* Fitton, J.G., Mahoney, J.J., Wallace, P. and

Saunders, A.D. (Eds.), Origin and Evolution of the Ontong Java Plateau. Geol. Soc. London, Spec. Publ., v.229, pp.151-178.

Fuster, J.M., Ibarrola, E. and Lopez-Ruiz, J. (1966) Volcanological and petrological study of the island of Lanzarote (Canary Islands). Estudios Geol., v.22, pp.185-200.

Fluegel, A. (2007) Glass viscosity calculation based on a global statistical modelling approach. Glass Technology: European Jour. Glass Sci. Tech., v.48, pp.13-30.

Genge, M.J., Price, G.D. and Jones, A.P. (1995) Molecular dynamics simulations of $CaCO_3$ melts to mantle pressures and temperatures: implications for carbonatite magmas. Earth Planet. Sci. Lett., v.131, pp.225-238.

Giberti, G. and Wilson, L. (1990) The influence of geometry on the ascent of magma in open fissures. Bull. Volcanol., v.52, pp.515-521.

Giordano, D., Russell, J.K. and Dingwell, D.B. (2008) Viscosity of magmatic liquids: a model. Earth Planet. Sci. Lett., v.271, pp.123-134.

Halls, H.C. and Fahrig, W.F. (1987) Dyke swarms and continental rifting: some concluding remarks. *In:* Halls, H.C. and Fahrig W.F. (Eds.), Mafic Dyke Swarms. Geol. Assoc. Canada Spec. Publ., v.34, pp.483-492.

Hack, A.C. and Thompson, A.B. (2011) Density and viscosity of hydrous magmas and related fluids and their role in subduction zone processes. Jour. Petrol., v.52, pp.1333-1362.

Hawkesworth, C., George, R., Turner, S. and Zellmer, G. (2004) Time scales of magmatic processes. Earth Planet. Sci. Lett., v.218, pp.1-16.

Huppert, H.E. and Sparks, R.S.J. (1985a) Cooling and contamination of mafic and ultramafic magmas during ascent through continental crust. Earth Planet. Sci. Lett., v.74, pp.371-386.

Huppert, H.E. and Sparks, R.S.J. (1985b) Komatiites I: eruption and flow. Jour. Petrol., v.26, pp.94-725.

Jankovics, M.E., Dobosi, G., Embey-Isztin, A., Kiss, B., Sági, T., Harangi, S. and Ntaflos, T. (2013) Origin and ascent history of unusually crystal-rich alkaline basaltic magmas from the western Pannonian Basin. Bull. Volcanol., v.75, pp.749-772.

Jankovics, M. E., Harangi, S., Németh, K., Kiss, B. and Ntaflos, T. (2015) A complex magmatic system beneath the Kissomlyó monogenetic volcano (western Pannonian Basin): evidence from mineral textures, zoning and chemistry. Jour. Volcanol. Geotherm. Res., v.301, pp.38-55.

Jing, Z. and Karato, S. (2012) Effect of H_2O on the density of silicate melts at high pressures: static experiments and the application of a modified hard-sphere model of equation of state. Geochim. Cosmochim. Acta,, v.85, pp.357-372.

Karki, B.B. Zhang, J. and Stixrude, L. (2013) First principles viscosity and derived models for MgO-SiO_2 melt system at high temperature. Geophys. Res. Lett., v.40, pp.94-99.

Kelley, S.P. and Wartho, J-A. (2000) Rapid kimberlite ascent and the significance of Ar-Ar ages in xenolith phlogopites. Science, v.289, pp.601-611.

Kerr, R.C. and Lister, J.R. (1991) The effects of shape on crystal settling and on the rheology of magmas. Jour. Geol., v.99, pp.457-467.

Klügel, A., Hansteen, T.H. and Schmincke, H.U. (1997) Rates of magma ascent and depths of magma reservoirs beneath La Palma (Canary Islands). Terra Nova, v.9, pp.117-121.

Le Bas, M.J., Le Maitre, R.W., Streckeisen, A. and Zanettin, B. (1986) A chemical classification of volcanic rocks based on the total alkali-silica diagram. Jour. Petrol., v.27, pp.745-750.

Leelanandam, C. (1989) The Prakasam alkaline province in Andhra Pradesh, India. Jour. Geol. Soc. India, v.34, pp.25-45.

Lindsay, J.M., Trumbull, R.B. and Siebel, W. (2005) Geochemistry and petrogenesis of late Pleistocene to Recent volcanism in southern Dominica, Lesser Antilles. Jour. Volcanol. Geotherm. Res., v.148, pp.259-294.

Lister, J.R. and Kerr, R.C. (1991) Fluid-mechanical models of crack propagation and their application to magma transport in dykes. Jour. Geophys. Res., v.96, pp.10049-10077.

Madhavan, V., Mallikharjuna Rao, J., Subrahmanyam, K., Krishna, S.G. and Leelanandam. C. (1989) Bedrock geology of Elchuru alkaline pluton, Prakasam district, Andhra Pradesh. *In*: Leelanandam, C. (Ed.), Alkaline Rocks. Mem. Geol. Soc. India, no.15, pp.189-205.

Madhavan, V. and Mallikharjuna Rao, J. (1990) Petrology of olivine basalt dyke of lamprophyre affinity at Uppalapadu, Prakasam District, Andhra Pradesh. Jour. Geol. Soc. India, v.36, pp.493-501.

Madhavan, V., Mallikharjuna Rao, J., Balaram, V. and Ramesh Kumar (1992) Geochemistry and petrogenesis of lamprophyres and associated dykes from Elchuru, Andhra Pradesh, India. Jour. Geol. Soc. India, v.40, pp.135-149.

Marsh, B.D. (1981) On the crystallinity, probability of occurrence, and rheology of lavas and magmas. Contrib. Mineral. Petrol., v.78, pp.85-98.

Mattsson, H.B. (2012) Rapid magma ascent and short eruption durations in the Lake Natron–Engaruka monogenetic volcanic field (Tanzania): a case study of the olivine melilititic Pello Hill scoria cone. Jour. Volcanol. Geotherm. Res., v.247-248, pp.16-25

McBirney, A.R. and Murase, T. (1984) Rheological properties of magmas. Annu. Rev. Earth Planet. Sci., v.12, pp.337-357.

McKenzie, D. (2000) Constraints on melt generation and transport from U-series activity ratios. Chem. Geol. v.162, pp.81-94.

Melnik, O. and Sparks, R.S.J. (2005) Controls on conduit magma flow dynamics during lava dome building eruptions. Jour. Geophys. Res., v.110**,** B02209, doi:10.1029/2004JB003183

Michaut, C. (2011) Dynamics of magmatic intrusions in the upper crust: theory and applications to laccoliths on earth and the moon. Jour. Geophys. Res., v.116, B5, doi**:** 10.1029/2010JB008108.

Michaut, C., Baratoux, D. and Thorey, C. (2013) Magmatic intrusions and deglaciation at mid-latitude in the northern plains of Mars. Icarus, v. 225, pp.602-613.

Mysen, B.O. (1988) Structure & Properties of Silicate Melts. Elsevier, Amsterdam, pp.354.

Nicholis, M.G. and Rutherford, M.J. (2004) Experimental constraints on magma ascent rate for the Crater Flat volcanic zone hawaiite. Geol. Soc. Amer., v.32, pp.489-492.

Nisbet, E.G., Cheadle, M.J., Arndt, N.T. and Bickle, M.J. (1993) Constraining the potential temperature of the Archaean mantle: a review of the evidence from komatiites. Lithos, v.30, 291-307.

Olson, J. and Pollard D.D. (1989) Inferring paleostresses from natural fracture patterns: a new method. Geology, v.17, pp.345-348.

Pearce, J.A., Baker, P.E., Harvey, P.K. and Luff, I.W. (1995) Geochemical evidence for subduction fluxes, mantle melting and fractional crystallization beneath the South Sandwich-Island Arc. Jour. Petrol., v.36, pp.1073-1109.

Peslier, A.H. and Luhr, J.F. (2006) Hydrogen loss from olivines in mantle xenoliths from Simcoe (USA) and Mexico: mafic alkalic magma ascent rates and water budget of the sub-continental lithosphere. Earth Planet. Sci. Lett., v.242, pp.302-319.

Peslier, A.H., Woodland, A.B. and Wolff, J.A. (2008) Fast kimberlite ascent rates estimated from hydrogen diffusion profiles in xenolithic mantle olivines from southern Africa. Geochim. Cosmochim. Acta, v.72, pp.2711-2722.

Petford, N. (2009) Which effective viscosity? Mineral. Mag., v.73, pp.167-191.

Petford, N., Lister, J.R. and Kerr, R.C. (1994) The ascent of felsic magmas in dykes. Lithos, v.32, pp.161-168.

Philpotts, A.R. (1990) Principles of Igneous and Metamorphic Petrology, Prentice-Hall of India, New Delhi, 498p.

Pinkerton, H. and Stevenson, R.J. (1992) Methods of determining the theological properties of magmas at subliquidus temperatures. Jour. Volcanol. Geotherm. Res., v.53, pp.47-66.

Pollard, D.D. and Muller, O.H. (1976) The effect of gradients in regional stress and magma pressure on the form of sheet intrusions in cross section. Jour. Geophys. Res., v.81, pp.975-984.

Pollard, D.D., Segall, P. and Delaney, P.T. (1982) Formation and interpretation of dilatant echelon cracks. Bull. Geol. Soc. Amer., v.93, pp.1291-1303.

Pollard, D.D., Delaney, P.T., Duffield, W.A. and Endo, E.T. (1983) Surface deformation in volcanic rift zones. Tectonophysics, v.94, pp.541-584.

Pollard, D.D. (1987) Elementary fracture mechanics applied to the structural interpretation of dykes. *In*: Halls, H.C. and Fahrig, W.F. (Eds.), Mafic Dyke Swarms. Geol. Assoc. Canada Spec. Paper., v.34, pp.5-24.

Price, S.E., Russell, J.K. and Kopylova, M.G. (2000) Primitive magma from the Jericho Pipe, N.W.T., Canada: constraints on primary kimberlite melt chemistry. Jour. Petrol., v.41, pp.789-808.

Price, R.C., Gamble, J.A., Smith, I.E.M., Stewart, R.B., Eggins, S. and Wright, I.C. (2005) An integrated model for the temporal evolution of andesites and rhyolites and crustal development in New Zealand's North Island. Jour. Volcanol. Geotherm. Res., v.140, pp.1- 24.

Rao, A.D.P., Rao, K.N. and Murthy, Y.G.K. (1987) Gabbro-anorthosite-pyroxenite complexes and alkaline rocks of Chimakurti-Elchuru area, Prakasam District, Andhra Pradesh. Records of Geol. Surv. India, v.116, pp.1-20.

Rathna, K., Vijaya Kumar, K. and Ratnakar, J. (2000) Petrology of the dykes of Ravipadu, Prakasam Province, Andhra Pradesh, India. Jour. Geol. Soc. India., v.55, pp.339-412.

Ratnakar, J. and Leelanandam, C. (1989) Petrology of alkaline plutons from the eastern and southern Peninsular India. *In:* Leelanandam, C. (Ed.), Alkaline Rocks. Mem. Geol. Soc. India., no.15, pp.145-176.

Ray, A., Hatui, K., Paul, D.K., Sen, G., Biswas, S.K. and Das, B. (2016) Mantle xenolith-xenocryst-bearing monogenetic alkali basaltic lava field from Kutch Basin, Gujarat, Western India: estimation of magma ascent rate. Jour. Volcanol. Geotherm. Res., v.312, pp.40-52.

Rogers, R.D. and Bird, D.K. (1987) Fracture propagation associated with dike emplacement at the Skaergaard intrusion, East Greenland**.** Jour. Struct. Geol., v.9, pp.71-86.

Rutherford, M.J. and Hill, P.M. (1993) Magma ascent rates from amphibole breakdown: experiments and the 1980-1986 Mount St. Helens eruptions. Jour. Geophys. Res., v.98, pp.19667-19685.

Russell, J.K., Porritt, L., Lavallee, Y. and Dingwell, D.B. (2012) Kimberlite ascent by assimilation-fuelled buoyancy. Nature, v.481, pp.352-356.

Sarkar, A. and Paul, D.K. (1998) Geochronology of the Eastern Ghats Precambrian Mobile Belt a review. Geol. Surv. India. Spec. Publ., v.44, pp.51-86.

Scarfe, C.M., Mysen, B.O. and Virgo, D. (1987) Pressure dependence of the viscosity of silicate melts. *In:* Mysen, B.O. (Ed.), Magmatic Processes: Physicochemical Principles. Geochem. Soc., Spec. Publ., v.1, pp.59-67.

Shaw, H.R. (1965) Comments on viscosity, crystal settling, and convection in granitic magmas. Amer. Jour. Sci., v.263, pp.120-152.

Shaw, H.R. (1972) Viscosities of magmatic silicate liquids: an empirical method of prediction. Amer. Jour. Sci., v.272, pp.870-893.

Shaw, H.R. (1980) The fracture mechanism of magma transport from the mantle to the surface. *In:* Hargraves, R.B. (Ed.), Physics of Magmatic Processes. Princeton University Press, Princeton, New Jersey, pp.201-264.

Sparks, R.S.J. (1993) Magma generation in the Earth. *In*: Hawkesworth C. and Wilson, C. (Eds.), Understanding the Earth. Cambridge University Press, Cambridge, pp.91-114

Sparks, R.S.J. (2003) Dynamics of magma degassing. Geol. Soc. London Spec. Publ., v.213, pp.5-22.

Sparks, R.S.J., Baker, L., Brown, R.J., Field, M., Schumacher, J., Stripp, G. and Walters, A. (2006) Dynamical constraints on kimberlite volcanism. Jour. Volcanol. Geotherm. Res., v.155, pp.18-48.

Spera, F.J. (1984) Carbon dioxide in petrogenesis III: role of volatiles in the ascent of alkaline magma with special reference to xenoliths-bearing mafic lavas. Contrib. Mineral. Petrol., v.88, pp.217-232.

Spera, F.J. (1986) Fluid dynamics of ascending magma and mantle metasomatic fluids. *In:* Menzies, M. and Hawkesworth, C. (Eds.), Mantle Metasomatism. Academic Press, London, pp.241-259.

Subba Rao, T.V., Bhaskar Rao, Y.J., Sivaraman, T.V. and Gopalan, K. (1989) Rb-Sr age and petrology of Elchuru alkaline complex: implications to alkaline magmatism in the Eastern Ghat Mobile Belt. *In:* Leelanandam, C. (Ed*.),* Alkaline Rocks. Mem. Geol. Soc. India., no.15, pp.207-223.

Taisne, B., Tait, S. and Jaupart, C. (2011) Conditions for the arrest of a vertical propagating dyke. Bull. Volcanol., v.73, pp.191-204.

Thomas, A.L. and Pollard, D.D. (1993) The geometry of echelon fractures in rock: implications from laboratory and numerical experiments. Jour. Struct. Geol., v.15, pp.323-334.

Ui, T., Kono, M., Hamano, Y., Monge, F. and Aota, Y. (1984) Reconstruction of a volcanic edifice using the dike swarm at Ocros, Peruvian Andes. Bull. Volcanol. Soc. Japan, v.29, pp. 285-296.

Upadhyay, D., Raith, M.M., Mezger, K. and Hammerschmidt, K. (2006) Mesoproterozoic rift-related alkaline magmatism at Elchuru, Prakasam Alkaline Province, SE India. Lithos, v.89, pp.447-477.

Vijaya Kumar, K. and Ratnakar, J. (2001) Petrogenesis of the Ravipadu gabbro pluton, Prakasam Alkaline Province, Andhra Pradesh. Jour. Geol. Soc. India, v.57, pp.113-140.

Vijaya Kumar, K., Frost, C.D., Frost, B.R. and Chamberlain, K.R. (2007) The Chimakurthi, Errakonda, and Upplapadu plutons, Eastern Ghats Belts, India: an unusual association of tholeiitic and alkaline magmatism. Lithos, v.97, pp.30-57.

Vijaya Kumar, K. and Leelanandam, C. (2008) Evolution of the Eastern Ghats Belt, India: a plate tectonic perspective. Jour. Geol. Soc. India, v.72, pp.720-749.

Vijaya Kumar, K. Ernst, W.G., and Leelanandam, C. (2011) Opening and closing of a Mesoproterozoic Ocean along the SE margin of India: textural, cathodoluminescence and SHRIMP analyses of zircon. Abstract V14B-07, Amer. Geophys. Union, Fall Meeting, San Francisco, USA.

Wada, Y. (1994) On the relationship between dike width and magma viscosity. Jour. Geophys. Res., v.99, pp.17743-17755.

Wartho, J-A. and Kelley, S.P. (2003) $^{40}Ar/^{39}Ar$ ages in mantle xenolith phlogopites: determining the ages of multiple lithospheric mantle events and diatreme ascent rates in southern Africa and Malaita, Solomon Islands. Geol. Soc. London Spec. Publ.**,** v.220, pp.231-248.

Whittington, A.G., Hellwig, B.M., Behrens, H., Joachim, B., Stechern, A. and Vetere, F. (2009) The viscosity of hydrous dacitic liquids: implications for the rheology of evolving silicic magmas. Bull. Volcanol., v.71, pp.185-199.

Wilson, L. and Head, J.W. (2007) An integrated model of kimberlite ascent and eruption. Nature, v.447, pp.53-57.

Wyllie, J.J., Voight, B. and Whitehead, J.A. (1999) Instability of magma flow from volatile-dependent viscosity. Science, v.285, pp.1883-1885.

Yamato, P., Tartese, R., Duretz, T. and May, D.A. (2012) Numerical modelling of magma transport in dykes. Tectonophysics, v.526-529, pp.97-109.

Zellmer, G.F., Hawkesworth, C.J., Sparks, R.S.J., Thomas, L.E., Harford, C.L., Brewer, T.S. and Loughlin, S.C. (2003) Geochemical evolution of the Soufrière Hills Volcano, Monserrat, Lesser Antilles volcanic arc. Jour. Petrol., v.44, pp.1349-1374.

Zimova, M. and Webb, S.L. (2006) The combined effects of chlorine and fluorine on the viscosity of alumina silicate melts. Geochim. Cosmochim. Acta, v.71, pp.1553-1562.

(Received: 20 June 2017; Revised form accepted: 1 September 2017)